Andrea Debnarova, Simone Techert, and Stefan Schmatz

Articles you may be interested in

Accurate small and wide angle x-ray scattering profiles from atomic models of proteins and nucleic acids
J. Chem. Phys. **141**, 22D508 (2014); 10.1063/1.4896220

On the role of the simplest S-nitrosothiol, HSNO, in atmospheric and biological processes
J. Chem. Phys. **139**, 234304 (2013); 10.1063/1.4840495

Coherent control of the isomerization of retinal in bacteriorhodopsin in the high intensity regime
J. Chem. Phys. **134**, 085105 (2011); 10.1063/1.3554743

Molecular structure determination from x-ray scattering patterns of laser-aligned symmetric-top molecules
J. Chem. Phys. **131**, 131101 (2009); 10.1063/1.3245404

Ab initio treatment of time-resolved x-ray scattering: Application to the photoisomerization of stilbene
J. Chem. Phys. **125**, 224101 (2006); 10.1063/1.2400231
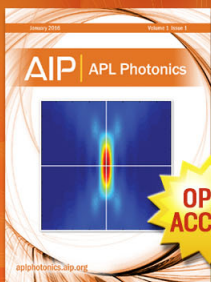
Computational studies of the x-ray scattering properties of laser aligned stilbene

Andrea Debnarova,[1] Simone Techert,[1,a)] and Stefan Schmatz[2,b)]

[1]*Max Planck Institute for Biophysical Chemistry, Göttingen, Germany*
[2]*Institut für Physikalische Chemie, Universität Göttingen, Germany*

The enhancement of the x-ray scattering signal from partially aligned molecular samples is investigated. The alignment properties of the studied molecular system are modeled based on the method of laser alignment. With the advances in the area of laser alignment of molecules, the application of this sample manipulation technique promises a great potential for x-ray scattering measurements. Preferential alignment of molecules in an otherwise amorphous sample leads to constructive interference and thus increases the scattering intensity. This enhances the structural information encoded in the scattering images and enables improved resolution in studies of reaction dynamics, as in this work is shown for the example of the photo-isomerization of stilbene. We demonstrate that the scattering signal is strongly influenced by the alignment axis. Even the most basic one-dimensional alignment offers significant improvement compared to the structural information provided by a randomly oriented sample. Although the signal is sensitive to the uncertainty in the alignment angle, it offers encouraging results even at realistic alignment uncertainties. © *2011 American Institute of Physics.*
[doi:10.1063/1.3523569]

I. INTRODUCTION

With the build-up of new x-ray sources the interest in their utilization for detailed measurements of the structure and dynamics of various molecular systems—including bio-molecules and their dynamical features—has naturally increased.[1] Already Neutze *et al.*[2] considered the implications which the combination of high intensity and short pulse lengths of the free electron laser (FEL) provides for structural studies; these authors evaluate the feasibility of structural measurements of samples consisting of a single molecule, while taking into account that Coulomb explosion occurs due to the high intensity of the laser pulse. Although this proposed technique avoids the problems concerning crystallization, which has been a necessity in structural studies using conventional x-ray sources, it also introduces new challenges for the experimentalists. Generally, one would prefer to study molecular systems and their chemical dynamics in their natural environments, e.g., in solution. To introduce a periodicity into such a system, various methods of alignment have been proposed[3–5] and experimentally performed[6] for small test systems.

The interest in manipulating the orientation of molecules in space originates from the studies of chemical reactions which in most cases depend on the mutual orientation of the reactants. One of the most promising methods emerging is the alignment under the influence of laser fields. A number of theoretical and experimental papers have been published in recent years on the laser-induced alignment of molecules[6–9] including a review of alignment techniques with the main focus on alignment in strong laser fields.[10]

The alignment of molecules by a laser field is based on the interaction of a strong nonresonant laser field with an induced molecular dipole moment. This interaction creates an energetic minimum for the alignment along the polarization axis of the field and so limits the free rotation of the molecules. Under these conditions, molecules *librate* in a limited angular range. The laser alignment technique is a fast emerging method of choice in experiments. It is assumed that the vibrational degrees of freedom can be neglected and the alignment depends only on the rotational degrees of freedom of the molecule.

For x-ray scattering, the degree of alignment is an important property since it introduces additional "periodicity" to an otherwise disordered system and thus enhances the characteristic details in the scattering signal.[11,12] As we will show, even the most basic one-dimensional (1D) alignment offers additional structural information in comparison to a completely amorphous sample. We talk about 1D alignment when the rotation about two of the axes of the molecule is hindered.[13] This simply means that the molecule can freely rotate around one axis, but not around the remaining axes. If alignment is initiated from a disordered state, the molecular orientation, however, is only determined up to 180° rotation with respect to the axes around which rotation is hindered. The reason is that the molecular polarizability tensor is symmetric with respect to inversion, and the aligning laser field does not distinguish between up and down orientation with respect to the alignment axis. 1D alignment provides a good compromise between added demands on the experimental setup and enhanced sample periodicity, and so increases constructive interference in the scattering signal. The x-ray scattering spectra of molecules investigated with 1D alignment provide the extra structural information necessary

---

a)Electronic mail: stecher@gwdg.de.
b)Electronic mail: sschmat@gwdg.de.

to study even relatively small structural changes and thus enable, for example, time-resolved studies of systems undergoing structural change. Even higher control over the periodicity in the sample provides the three-dimensional (3D) alignment and orientation control. This would to some extent simulate single-molecule scattering, however, it poses a much more difficult problem than simple 1D alignment. Recently, time-resolved electron diffraction[14–16] deals with that problem.[17–19]

In recent years a number of papers concerning various methods of x-ray imaging applied to aligned systems has been published, dealing with small test systems such as Br_2.[20,21] In this work, we study whether sample alignment is a suitable option for x-ray scattering studies of relatively small organic systems with the emphasis on time-resolved problems. The chosen model process is the photo-isomerization of stilbene, as a prototypical photo-induced process.[22,23] Generally, photo-induced processes are of high importance in biochemistry;[24] practically they are being assessed in the growing field of organic electronics.[25] Understanding these processes is essential for their successful application in the various branches of material science. Furthermore, in photophysics, processes hidden to spectroscopic measurements occur, though measurement of the electron density and its time evolution, respectively, are still attainable.

As an additional motivation for the interest in aligned samples we should add that while the current FEL, with pulse lengths on the level of femtoseconds, promises many interesting applications for measurements, methods for achieving even shorter pulse lengths, on the level of attoseconds, have been proposed.[26,27] A side effect of the pulse shortening is, however, a decrease in the pulse intensity, which would not be sufficient for single molecule measurements. On the other hand, it provides an incentive to look into the feasibility of time-resolved measurements of aligned samples.

II. THEORY AND METHODOLOGY

The well-known expression[28] for the x-ray scattering intensity as a Fourier transformation of the electron density can be described in terms of the differential scattering cross section. For the differential scattering cross section in elastic scattering, it holds

$$\frac{d\sigma}{d\Omega} \propto \left| \left\langle f \left| \sum_j \exp(i\mathbf{q} \cdot \mathbf{r}_j) \right| i \right\rangle \right|^2, \tag{1}$$

where $|f\rangle$ and $|i\rangle$ denote the wave functions of the final and initial state, respectively, and $\mathbf{r}_j$ are the electronic coordinates of atom j. In the case of x-ray scattering and diffraction, the initial state $|i\rangle$ of the molecule corresponds to the final state, the radiation potential does not cause any excitations. For a molecule, these wave functions include an electronic (coordinates $\mathbf{r}$) and a nuclear (coordinates $\mathbf{R}$) part, and within the Born-Oppenheimer approximation are written us

$$\Phi(\mathbf{R}, \mathbf{r}) = \Psi_{\text{el}}(\mathbf{r}|\mathbf{R})\chi_{\text{nu}}(\mathbf{R}), \tag{2}$$

with Ψ_{el} being implicitly $\mathbf{R}$-dependent, and χ_{nu} being the vibrational wave function, which in the harmonic approxima-

tion has the form $\chi_{\text{nu}}(Q_1, \ldots, Q_N) = \prod_{j=1}^{N} \xi_j(Q_j)$ with N denoting the internal nuclear degrees of freedom and Q_j being a normal coordinate. The use of this approach helps to clarify the influence of the molecular motion on the differential cross section and the scattering intensity.

The main term in Eq. (1) can be expanded as

$$\langle f | \exp(i\mathbf{q} \cdot \hat{\mathbf{r}}) | i \rangle$$

$$= \int \xi_1^*(Q_1) \cdots \xi_N^*(Q_N)\Psi_{\text{el}}^*(\mathbf{r}|\mathbf{Q})(\exp(i\mathbf{q} \cdot \hat{\mathbf{r}}))$$

$$\times \xi_1(Q_1) \cdots \xi_N(Q_N)\Psi_{\text{el}}(\mathbf{r}|\mathbf{Q}) \, dQ_1 \cdots dQ_N d\mathbf{r}$$

$$= \int |\xi_1(Q_1)|^2 \cdots |\xi_N(Q_N)|^2 \, dQ_1 \cdots dQ_N$$

$$\times \int \rho(\mathbf{r}|\mathbf{Q}) \exp(i\mathbf{q} \cdot \mathbf{r}) \, d\mathbf{r}, \tag{3}$$

where $\hat{\mathbf{r}}$ denotes the electron position operator and $\rho(\mathbf{r}|\mathbf{Q})$ is the implicity $\mathbf{R}$-dependent electron density.

In many practical cases some vibrational modes are strongly confined around an equilibrium position Q_j^0. By substituting the wave functions of these modes by the delta function $\xi_j(Q_j) = \delta_{Q_j^0}(Q_j)$ these modes can be easily integrated out of the expression by substituting the corresponding dependence on the vector $\mathbf{Q}$ with the positions Q_j^0 in the electron density term $\rho(\mathbf{r}|\mathbf{Q})|_{Q_j=Q_j^0}$.

To be able to deal with Eq. (3) one has to consider the implicit dependence of the electron density on the nuclear degrees of freedom. From quantum chemical calculations one obtains a set of $\rho(\mathbf{r})$, each corresponding to a different $\mathbf{Q}$ rather than an explicit function $\rho(\mathbf{r} | \mathbf{Q})$. From this, it follows that we have to deal with the vibrational degrees of freedom through numerical integration. A sufficiently small number of vibrational modes m which are considered to have an effect on the scattering intensity can be assessed by numerical integration and the differential cross section can be expressed in the form

$$\frac{d\sigma}{d\Omega} \propto \left| \int |\xi_1(Q_1)|^2 \cdots |\xi_m(Q_m)|^2 \, \mathcal{F}[\rho(\mathbf{r}|\mathbf{Q})] \, dQ_1 \cdots dQ_m \right|^2$$

$$= \left| \sum_{k_1} \Delta Q_1 \cdots \sum_{k_m} \Delta Q_m \, p_1(k_1\Delta Q_1) \cdots p_m(k_m\Delta Q_m) \right.$$

$$\left. \times \mathcal{F}[\rho(\mathbf{r}|k_1\Delta Q_1, \ldots, k_m\Delta Q_m)] \right|^2, \tag{4}$$

where $\mathcal{F}[\rho(\mathbf{r}|\mathbf{Q})]$ denotes the Fourier transformation of the electron density at a given point $\mathbf{Q}$ in the space of vibrational coordinates and the indices $k_1, \ldots, k_m$ run through the discretized probability distribution functions of the vibrational wave functions $p_j(Q_j) = |\xi_j(Q_j)|^2$. In practice, the number of contributing modes m stays small because mainly the weakly confined ones significantly change the overall intensity.

Having the implicit $\mathbf{Q}$-dependence of the electron density in mind, we can now move on to studying its influence on the time-dependence of x-ray scattering. This enters the equations through the nuclear degrees of freedom as $\xi(\mathbf{Q}, t)$

and $p_j(Q_j, t) = |\xi_j(Q_j, t)|^2$ and thus also the electron density $\rho(\mathbf{r}|\mathbf{Q}, t)$.

Scattering from a random distribution of molecular orientations in gaseous or liquid samples can be assessed straightforwardly by summing the intensity contributions from all molecules in the sample, which practically means integrating Eq. (4) over all angles in spherical coordinates, for all possible orientations of the molecules in the sample:

$$
\frac{d\sigma}{d\Omega} \propto \frac{1}{4\pi q^2} \int \left| \sum_{k_1} \Delta Q_1 \cdots \sum_{k_m} \Delta Q_m \, p_1(k_1 \Delta Q_1) \cdots \right.
$$

$$
\left. \times \, p_m(k_m \Delta Q_m) \, \mathcal{F}(\mathbf{q})[\rho] \right|^2 \sin\theta \, d\theta \, d\varphi
$$

$$
= \frac{1}{2q^2} \int |f(\mathbf{q})|^2 \, \sin\theta \, d\theta. \tag{5}
$$

Due to this integration, information about the structure is lost, the intensity no longer depends on the directions of the scattering vector $\mathbf{q}$ but only on its length q. To boost the structure characteristic part of the scattering intensity distribution, which is the important part of the signal used to identify the molecular structure of the system under study, one has to introduce periodicity into the system, as, e.g. is the case for a crystal. In the case of gaseous samples, this can be done through one of the methods of molecular orientation, for example, through a magnetic field or a laser field. By doing so we generally arrive at an ensemble of molecules with a preferred orientation of their molecular axes with respect to an external coordinate system, which corresponds to the external alignment field. The efficiency of the achieved alignment is characterized by a probability distribution of the uncertainty of the angle between the molecular axis and the external alignment field axis.

To study a system of aligned identical molecules, we have to consider the properties of the Fourier transformation with respect to an arbitrary rotation of the function $f(\mathbf{r})$ that is transformed. Any rotation of an object in 3D space can be constructed from three sequential rotations with respect to the Cartesian coordinate system axes x, y and z, which is mathematically expressed by sequential application of the rotation matrices $\hat{R}_x(\alpha)$, $\hat{R}_y(\beta)$, $\hat{R}_z(\gamma)$ corresponding to the Euler rotation angles α, β and γ. The Fourier transformation of a rotated function is then given by

$$
\mathcal{F}(\mathbf{k})[f(\hat{R}_z(\gamma)\hat{R}_y(\beta)\hat{R}_x(\alpha)\mathbf{r})]
$$

$$
= \int f(\hat{R}_z(\gamma)\hat{R}_y(\beta)\hat{R}_x(\alpha)\mathbf{r})e^{-i\mathbf{k}\mathbf{r}} \, d^3\mathbf{r}. \tag{6}
$$

Due to the consecutive application of the rotation matrices to the function $f(\mathbf{r})$, we can constrain the evaluation to one rotation $\hat{R}(\alpha)$ and simplify the integral to $\int f(\hat{R}(\alpha)\mathbf{r})e^{-i\mathbf{k}\mathbf{r}}d^3\mathbf{r}$. We apply the substitution $\mathbf{u} = \hat{R}(\alpha)\mathbf{r}$ and consider the back substitution $\mathbf{r} = \hat{R}(-\alpha)\mathbf{u}$ and the property $\hat{R}^T(\alpha) = \hat{R}(-\alpha)$ from which follows that $\mathbf{k} \cdot (\hat{R}(\alpha)\mathbf{r}) = (\hat{R}(-\alpha)\mathbf{k}) \cdot \mathbf{r}$. The Fourier transformation of the rotated

function is then

$$
\int f(\hat{R}(\alpha)\mathbf{r})e^{-i\mathbf{k}\cdot\mathbf{r}} \, d^3\mathbf{r} = \int f(\mathbf{u})e^{-i\mathbf{k}\cdot(\hat{R}(-\alpha)\mathbf{u})} \, d^3\mathbf{u}
$$

$$
= \int f(\mathbf{u})e^{-i(\hat{R}(\alpha)\mathbf{k})\cdot\mathbf{u}} \, d^3\mathbf{u}, \tag{7}
$$

from which we can conclude that for the general expression for the Fourier transformation of a rotated function, it holds:

$$
\mathcal{F}(\mathbf{k})[f(\hat{R}_z(\gamma)\hat{R}_y(\beta)\hat{R}_x(\alpha)\mathbf{r})]
$$

$$
= \mathcal{F}(\hat{R}_z(\gamma)\hat{R}_y(\beta)\hat{R}_x(\alpha)\mathbf{k})[f(\mathbf{r})]. \tag{8}
$$

Let us now consider a system of N identical molecules aligned with respect to their molecular axis with a probability distribution $p(\alpha)$ of the uncertainty in the alignment angle α. In order to maintain clarity and simplicity of the expressions, in the following the molecular wave function contribution to the total scattering will be omitted. An ensemble of aligned identical molecules with electron density $\rho(\mathbf{r})$ can be expressed as $\sum_{i=1}^{N} \rho(\hat{R}(\alpha_i)\mathbf{r})$ and the total differential cross section as a sum over the contributions from all molecules is given by

$$
\frac{d\sigma}{d\Omega} \propto \sum_{i=1}^{N} c(\alpha_i)|\mathcal{F}(\mathbf{q})[\rho(\hat{R}(\alpha_i)\mathbf{r})]|^2
$$

$$
= \sum_{i=1}^{N} c(\alpha_i)|\mathcal{F}(\hat{R}(\alpha_i)\mathbf{q})[\rho(\mathbf{r})]|^2
$$

$$
= \int p(\alpha)|\mathcal{F}(\hat{R}(\alpha)\mathbf{q})[\rho(\mathbf{r})]|^2 \, d\alpha, \tag{9}
$$

where $c(\alpha_i) > 0$ are the probability distribution coefficients with $\sum_{i=1}^{N} c(\alpha_i) = 1$. For large ensembles it is more appropriate to use a probability distribution $p(\alpha)$ with $\int p(\alpha)d\alpha = 1$.

Using the expressions presented in this section, the x-ray scattering intensities can be studied in space and time, without neglecting either realistic electron density distribution or vibrational degrees of freedom.

III. X-RAY SCATTERING ON ALIGNED SYSTEMS

In the case of the so-called 1D alignment (when the molecule can freely rotate around one axis) we deal with a straightforward integration in one rotational degree of freedom where one can conveniently include the uncertainty in confinement in θ with the probability distribution of the uncertainty $p(\theta)$ as

$$
I(k, \theta) = \frac{1}{2\pi} \int_0^\pi p(\theta) \sin\theta \, d\theta \int_0^{2\pi} |\mathcal{F}_{k,\theta,\varphi}[\rho(\mathbf{r})]|^2 d\varphi. \tag{10}
$$

As the calculated scattering intensity maps presented in this work show, the 1D alignment offers a significant improvement on the information about the geometry of the studied sample compared to a sample with random orientations. The uncertainty in the alignment angle θ is an important parameter. We chose to approximate the angular uncertainty distribution by a the Gaussian function, $\exp(-\alpha\theta^2)$.
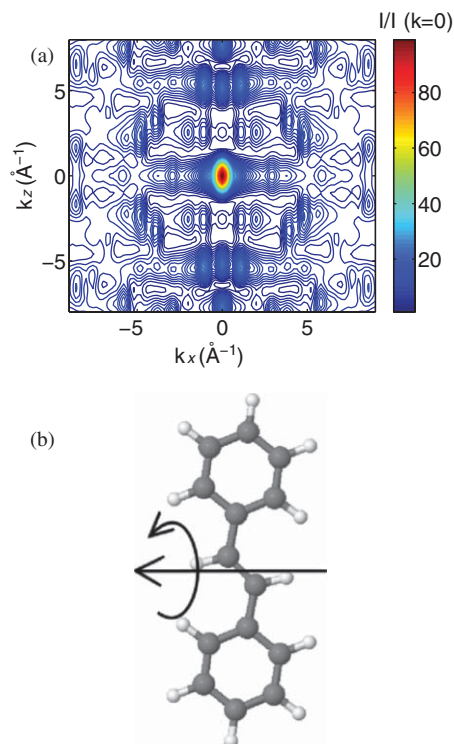
FIG. 1. (a) One-dimensional alignment of *trans*-stilbene with the alignment axis with 0° uncertainty in alignment perpendicular to the principal moment of inertia axis. (b) Molecule with the alignment axis around which it can rotate freely. Both projections are representative.

The most notable property of the 1D alignment is the dependence of the spectra on the alignment axis. Figures 1 and 2 show the 1D alignment scattering intensities of stilbene with respect to different alignment axes. The difference in the scattering spectra is significant. This is a promising feature since the principal polarizability axes, which coincide with the laser alignment axes, can be modified by attaching polarizable groups to the molecule. It should be pointed out that the effective degree of alignment can be enhanced in *trans*-stilbene when adding a polarizable residue like a bromo unit onto the para-position of the phenyl moiety (or by starting the investigations of the photo-isomerization from the reactant side, cis-stilbene). Moreover, strong permanent dipole moments are generated by such substitutions.

Keeping the alignment axis constant, we can show the importance of the precision in the alignment. Figure 3 displays the same alignment geometry as in Fig. 2, but with variation of the uncertainty in the alignment axis of 0°, 10°, 20°, and 30°, respectively. Similarly, Fig. 4 depicts the influence of the changing uncertainty of the alignment axis on the scattering spectra of aligned cis-stilbene. The strong scattering features of the well-aligned molecules fast diminish with growing uncertainty in the alignment angle. However, even the uncertainty distribution with the FWHM of 30° still offers a scattering spectrum that is much improved compared to a fully spherically symmetric scattering spectrum of a sample with randomly oriented molecules. In the experiments with the 1D laser alignment reported in Ref. 13, the smallest $\Delta\theta$ values achieved are in the range of about 20°.

Theoretically, the 3D alignment offers the best structural resolution of the studied sample. The expression for the inten-

sity distribution including the uncertainty in the alignment $\Delta\theta$ and $\Delta\varphi$ and the probability distributions of the uncertainty, $p_1(\theta)$ and $p_2(\varphi)$, is given by

$$I(k,\theta) = \int_0^\pi p_1(\theta)\sin\theta d\theta \int_0^{2\pi} p_2(\varphi)|\mathcal{F}_{k,\theta,\varphi}[\rho(\mathbf{r})]|^2 d\varphi. \quad (11)$$

Illustrative examples of scattering intensities with 3D alignment coincide with the single-molecule scattering examples and can be found in Ref. 29 on x-ray scattering from stilbene.

IV. TIME-RESOLVED SCATTERING ON ALIGNED STILBENE

Scattering on aligned samples gives information about the electron density projection on the alignment axis. This offers a number or interesting opportunities for measurements. Additionally, if one could change the polarizability axis of the molecule one could observe different projections of the density and so to some extent focus on the area of interest— the maximum density change corresponding to the observed process.

As shown in Sec. III, the 1D alignment provides additional structural information about the imaged object compared to a randomly oriented sample. In this section we
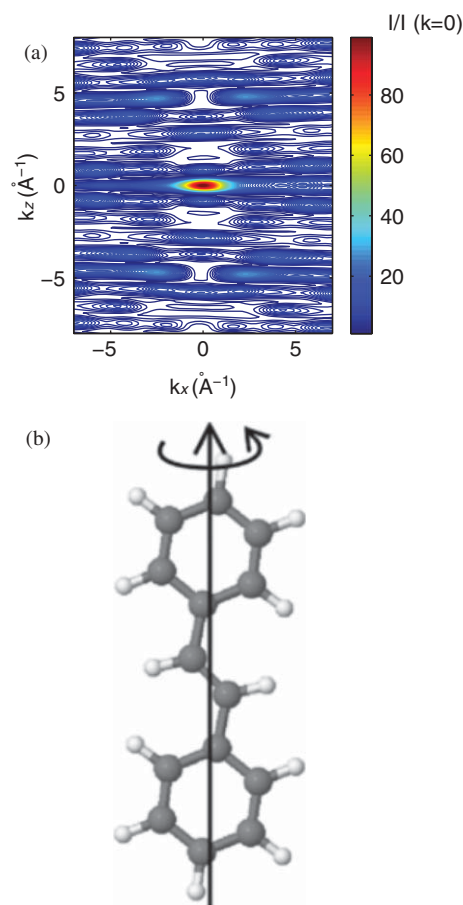

FIG. 2. (a) One-dimensional alignment of *trans*-stilbene with the alignment axis with 0° uncertainty in alignment equal to the principal moment of inertia axis. (b) Molecule with the alignment axis around which it can rotate freely. Both projections are representative.
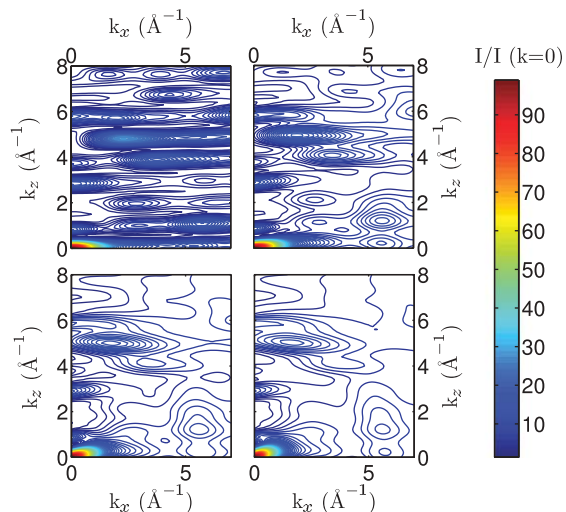
FIG. 3. Scattering from *trans*-stilbene with changing uncertainty in alignment; top-left with 0°; top-right with 10°; bottom-left with 20° and bottom-right with 30° uncertainty in alignment.

FIG. 5. Total scattering intensity during the isomerization of stilbene with 1D alignment (top) and in a randomly oriented ensemble (bottom).

evaluate whether this information is sufficient to follow time-dependent processes. We will focus on 1D alignment which poses the lowest experimental demands. In the following, in place of the time-scale of the photo-isomerization process we use the change of the dihedral angle during the process. The relation between these two variables is obvious; the impact on the scattering intensity is better described in terms of changes in geometry.

The photo-isomerization of stilbene is a nonradiative process due to the conical intersection between the ground state and the S_1 state potential energy surfaces (PESs). After absorption of a UV photon *trans*-stilbene is excited from the electronic ground state (^1A_g) to the first excited state (^1B_u). There is only a small barrier in the S_1 state between the Franck–Condon state and the conical intersection. After crossing this barrier, the process continues over the conical intersection ending up in the *cis*- or *trans*-conformation of the
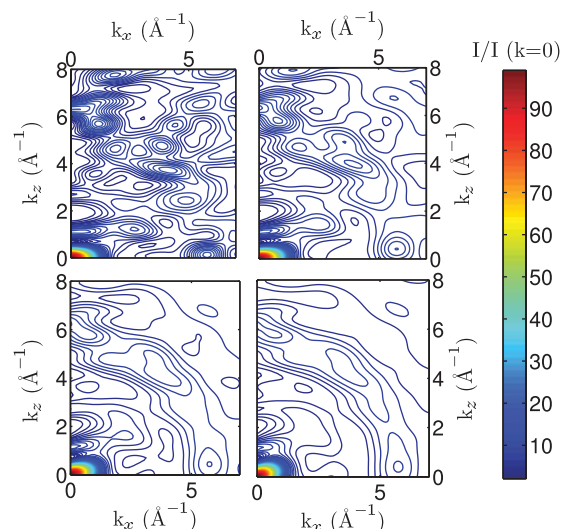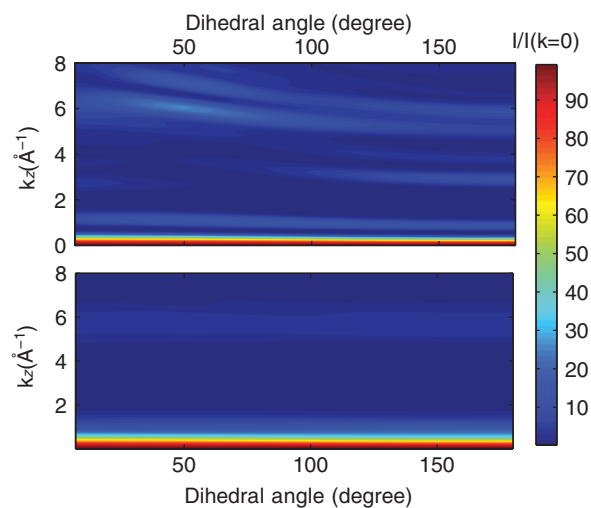
electronic ground state. The PES and molecular geometries are taken from our previous work.[26, 29]

The calculations start in the trans-geometry when the molecular ensemble is aligned with respect to the principal moment of inertia axis. To provide a comparison between the spectra of 1D aligned and randomly oriented molecules, we focus on the intensity along the $I_z = I(k_x = 0)$ line in the spectra of the 1D aligned system. The resulting 1D aligned time-resolved I_z spectra together with the randomly oriented molecular system counterparts are depicted in Figs. 5–7 and they show highest asymmetry in the scattering pattern. Figure 5 shows the comparison of the total intensities, while Fig. 6 gives the difference intensities between the trans-geometry and the geometry with the given dihedral angle; Fig. 7 displays the intensity difference between two consecutive geometries with a dihedral angle difference of 10°. In the aligned case the system has an uncertainty of alignment of 20° which will lead to some kind of smearing out of signal.

FIG. 4. Scattering from *cis*-stilbene with changing uncertainty in alignment; top-left with 0°; top-right with 10°; bottom-left with 20° and bottom-right with 30° uncertainty in alignment.
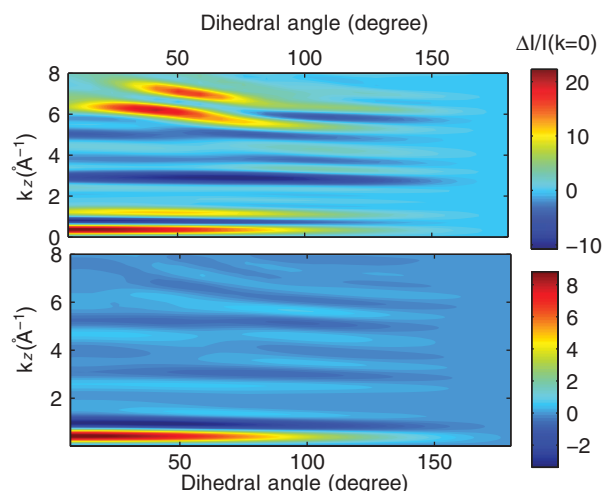

FIG. 6. Intensity difference between the scattering intensity of *trans*-stilbene and a stilbene geometry with a given dihedral angle with alignment (top) and in a randomly oriented ensemble (bottom).
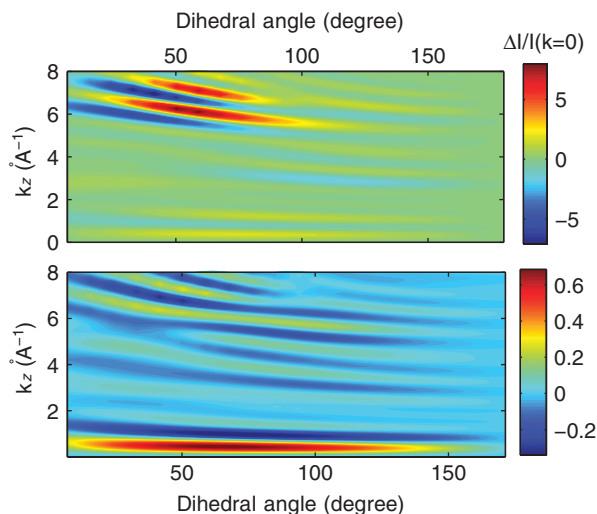
FIG. 7. Scattering intensity difference between two subsequent geometries, with a 10 degree dihedral angle step, with alignment (top) and in a randomly oriented ensemble (bottom).

As we will explain in Sec. V, the rotational dephasing of *cis*- and *trans*-stilbene can be forced to be much slower than the isomerization process itself by using a nanosecond alignment laser. Then, the difference in the alignment between the cis and trans state of stilbene leads to a modification in the final x-ray difference map but will not change the general conclusion which can be drawn from the present work.

In the simulation the alignment axis remains the principal moment of inertia axis at any given time. Since we want to examine the sensitivity of the 1D scattering spectra to the geometry change, we chose 18 equidistant geometry-change steps on the simplified minimum energy path on the PES, which corresponds to about $10°$ change of the dihedral angle per step. Experimentally, for keeping alignment "alive" during the photochemical process of isomerization, three laser systems need to be coupled in: a femtosecond laser to initiate the isomerization reaction, a nanosecond laser to align stilbene in the laboratory coordinate system, and an ultrafast x-ray pulse (FEL pulse) to probe the structure of the system. The long nanosecond pulses of the alignment laser guarantee an alignment longer than the isomerization processes (which in maximum takes some picoseconds). This experimental configuration prevents against the loss of degree of alignment through dephasing, which in turn could lead to a change of the radial distribution of intensity. For the very unlikely case that in real space the rotation of the whole molecule through dephasing has the same spatial consequences as isomerization, the scattering signal changes would become indistinguishable.

Figures 5–7 show relatively strong signal changes in the case of the aligned system even when we focus just on the 1D I_z intensity. As can be seen, even the reduced I_z intensity 1D scattering maps lead to an increase of bandwidth resolution (in $\Delta k/k$) allowing for a more detailed monitoring of structural changes compared to the scattering pattern of randomly oriented molecules. In comparison to the randomly oriented sample data, the aligned data show a bandwidth resolution enhancement especially in the geometry range between the

cis-conformation and the conformation with a dihedral angle of about $120°$. This best can be seen in Fig. 6.

In the case of the scattering differences between two consecutive steps (as shown in Fig. 7) changes in the intensity have a direct implication for the possible time-resolution of the scattering experiment. If we focus on the graphically less resolved region in the smaller k-range (up to about 4 Å^{-1}) two pairs of major maxima and minima with absolute values of about 2% can be observed. The first is a minimum at about $k = 1$ Å^{-1} which is present in all the angular range of the photo-isomerization geometry changes, reaching its maximum absolute values in the dihedral angular range from about $20°$ to $120°$, broadening towards the smaller dihedral angle— with the continuing photo-isomerization towards the cis-state. The second significant minimum in the smaller k-range is at about $k = 3$ Å^{-1} but in comparison to the first one it is more confined to the dihedral angular range reaching its maximum absolute value in the range from $90°$ to $140°$. Even more confined in the dihedral angular range are two maxima, the first of which appearing at about $k = 0.5$ Å^{-1} between $40°$ to $110°$, and the second at about $k = 1.2$ Å^{-1} confined to $70°$ to $100°$ in the dihedral angular range. In comparison to this, the intensity changes between two consecutive geometry steps in the case of the randomly oriented system are small in all dihedral angular ranges reaching a maximum of only about 0.6%. This means that a time-resolved measurement has much better prospects when measuring 1D aligned samples in comparison to a measurement with a randomly oriented system.

V. CONCLUSIONS

One-dimensional alignment offers a significant improvement over the structural information provided by a randomly oriented sample. While three-dimensional alignment is experimentally very demanding, especially having in mind the necessary concentration of the aligned molecules, the 1D alignment is slightly less of a challenge and so a good candidate especially in the area of time-dependent scattering measurements.

Since 1D alignment offers improved scattering intensity information compared to a randomly oriented system, it opens the opportunity for better time-resolved x-ray scattering measurements. At the same time, although it is sensitive to the uncertainty in the alignment angle, it offers good results even at a realistic alignment uncertainty distribution of $20°$ full width at half maximum.

It is necessary to look at the importance of the alignment axis on the scattering spectra. In the test case of stilbene, the alignment axis was chosen to be the principal axis of the moment-of-inertia tensor of the molecule. This is just a test axis used to study the alignment properties. In reality, the alignment axis is the principal axis of the polarizability tensor. As the molecular geometry changes during the isomerization process, the alignment axis changes accordingly, which virtually enhances the possible information provided by the scattering signal.

As we mentioned before, the spectrum of the 1D aligned system basically provides the information about the electron density projected onto the alignment axis. Therefore,

theoretically, by changing the alignment axis one could choose the projection with most pronounced density change during the observed process. If we introduced suitable methods of tagging and determining the alignment axis, this would give us the opportunity to study the molecule with respect to different axes and so possibly focus on the electron density area of interest.

The possible 3D alignment and orientation would bring the scattering experiment closer to single-molecule scattering conditions. However, this is a much more difficult experimental task, whereas the 1D alignment significantly improves the scattering resolution between geometrically close structures. This could contribute to vital enhancement of the time-resolved structural dynamics scattering measurements.

ACKNOWLEDGMENTS

[1] T. Tschentscher, Chem. Phys. **299**, 271 (2004).
[2] R. Neutze, R. Wouts, D. van der Spoel, E. Weckert, and J. Hajdu, Nature **406**, 752 (2000).
[3] T. Seideman, J. Chem. Phys. **103**, 7887 (1995).
[4] T. Seideman, Phys. Rev. Lett. **83**, 4971 (1999).
[5] T. Seideman, J. Chem. Phys. **115**, 5965 (2001).
[6] J. J. Larsen, H. Sakai, C. P. Safvan, I. Wendt-Larsen, and H. Stapelfeldt, J. Chem. Phys. **111**, 7774 (1999).
[7] S. S. Viftrup, V. Kumarappan, S. Trippel, and H. Stapelfeldt, Phys. Rev. Lett. **99**, 143602 (2007).
[8] R. Tehini and D. Sugny, Phys. Rev. A **77**, 023407 (2008).
[9] A. Pelzer, S. Ramakrishna, and T. Seideman, J. Chem. Phys. **129**, 134301 (2008).
[10] H. Stapelfeldt and T. Seideman, Rev. Mod. Phys. **75**, 543 (2003).
[11] M. Ben-Num, T. J. Martínez, P. M. Weber, and K. R. Wilson, Chem. Phys. Lett. **262**, 405 (1996).
[12] S. Techert and S. Schmatz, Z. Phys. Chem. **216**, 575 (2002).
[13] H. Stapelfeldt, Eur. Phys. J. D **26**, 15 (2003).
[14] J. C. Williamson, J. Cao, H. Ihee, H. Frey, and A. H. Zewail, Nature **386**, 159 (1997).
[15] B. J. Siwick, J. R. Dwyer, R. E. Jordan, and R. J. Miller, Science **302**, 1382 (2003).
[16] T. van Oudheusden, E. F. de Jong, S. B. van der Geer, W. P. E. M. Opt Root, and O. J. Luiten, J. Appl. Phys. **102**, 093501 (2007).
[17] P. Reckenthaeler, M. Centurion, W. Fuss, S. Trushin, F. Krausz, and E. Fill, Phys. Rev. Lett. **102**, 213001 (2009).
[18] K. Lee, D. Villeneuve, P. Corkum, A. Stolow, and J. Underwood, Phys. Rev. Lett. **97**, 173001 (2006).
[19] J. Cardoza, C. Dudek, R. Mawhorter, and P. Weber, Chem. Phys. **299**, 307 (2004).
[20] P. J. Ho and R. Santra, Phys. Rev. A **78**, 053409 (2008).
[21] P. J. Ho, M. R. Miller, and R. Santra, J. Chem. Phys. **130**, 154310 (2009).
[22] G. Busse, T. Tschentscher, A. Plech, M. Wulff, B. Frederichs and S. Techert, Faraday Discuss. **A22**, 105 (2003).
[23] S. Techert, A. Wiessner, S. Schmatz and H. Staerk, J. Phys. Chem. B **105**, 7579 (2001).
[24] A. S. F. Ramos and S. Techert, Biophys. J. **89**, 1990 (2005).
[25] N. K. Petrov, M. N. Gulakov, M. V. Alfimov, G. Busse, B. Frederichs, and S. Techert, J. Phys. Chem. A **107**, 6341 (2003).
[26] A. A. Zholents and M. S. Zolotorev, New J. Phys. **10**, 025005 (2008).
[27] E. L. Saldin, E. A. Schneidmiller, and M. V. Yurkov, Phys. Rev. ST Accel. Beams **9**, 050702 (2006).
[28] B. E. Warren, *X-Ray Diffraction* (Addison-Wesley, Reading, MA, 1969).
[29] A. Debnarova, S. Techert, and S. Schmatz, J. Chem. Phys. **125**, 224101 (2006).